Proceedings of Ninth World Conference on Earthquake Engineering
August 2-9, 1988, Tokyo-Kyoto, JAPAN (Vol.VIII)

SC-7

APPLICATIONS OF RECURSIVE EVALUATION OF INTERACTION FORCES OF UNBOUNDED SOIL IN NONLINEAR SOIL-STRUCTURE-INTERACTION ANALYSIS

John P. WOLF[1] and Masato MOTOSAKA[2]

[1] Institute of Hydraulics and Energy, Department of Civil Engineering, Swiss Federal Institute of Technology, Lausanne, CH-1015 Lausanne, Switzerland

[2] Kobori Research Complex, Kajima Corporation, Tokyo 163, Japan

SUMMARY

After reviewing the recursive evaluation of the interaction forces based on the flexibility formulation, two applications are presented. In the first, the dynamic-flexibility coefficients in the frequency domain are approximated as ratios of two polynomials, and in the second, the dynamic-flexibility coefficients in the time domain are divided into segments which are approximated. Both procedures lead to highly accurate results. Thanks to the significant reduction in computational effort and in storage requirement, it is possible to perform realistic nonlinear soil-structure-interaction analysis with many degrees of freedom in the time domain.

INTRODUCTION

The basic equation of motion of the substructure method to analyse the interaction of a nonlinear structure including an irregular adjacent bounded soil region and the unbounded linear soil is derived in Ref.1. Based on the flexibility formulation, the displacement interaction-force relationship of the unbounded soil with excavation is formulated in the form of a convolution integral as (Fig.1)

$$\{u_b^t(t)\}-\{u_b^g(t)\}=\int_0^t [F_{bb}^g(t-\tau)]\{R_b(\tau)\}d\tau \tag{1}$$

$\{u_b^t(t)\}$ and $\{u_b^g(t)\}$ denote the total displacement and the generalized scattered displacement on the structure-soil interface (u_b, w_b in the two-dimensional case illustrated in Fig.1). $\{u_b^t(t)\}-\{u_b^g(t)\}$ represents the relative displacement $\{u_b(t)\}$. $\{R_b(t)\}$ is the interaction forces (P_b, R_b in Fig.1) and $[F_{bb}^g(t)]$ denotes the dynamic-stiffness coefficients of the soil (system ground) in the time domain. $[F_{bb}^g(t)]$ is the Fourier transform of the corresponding value in the frequency domain $[F_{bb}^g(\omega)]$, which is equal to the inverse of the familiar dynamic-stiffness coefficients $[S_{bb}^g(\omega)]$. The subscript b and the superscripts t, g are dropped for the sake of conciseness in the following sections.

The computational procedure involving temporal discretization to incorporate the flexibility formulation of the unbounded soil into the direct stiffness method of the structure is described in Ref.1.

RECURSIVE EVALUATION OF CONVOLUTION INTEGRAL FOR FLEXIBILITY FORMULATION

As the boundary condition in eq.1 is global in time (and space); i.e. the interaction forces in all nodes on the structure soil interface from the start of the excitation contribute to the displacement, the computational effort and the storage requirement are significant. To be able to achieve a reduction, the convolution integrals are evaluated recursively at each time station. In this method, the displacements $\{u\}_n$ at time $t=n\Delta t$ are computed from the nth interaction forces $\{R\}_n$ and the M and L most recent past values of the displacements and interaction forces, respectively. To evaluate a typical convolution integral appearing in eq.1, written as

$$\{u\}_n = \int_0^t [F(t-\tau)]\{R(\tau)\}d\tau \qquad (2)$$

the recursive formulation leads to

$$\{u\}_n = \sum_{i=1}^{M} [a]_i \{u\}_{n-i} + \Delta t \sum_{i=0}^{L} [b]_i \{R\}_{n-i} \qquad (3)$$

$[a]_i$ and $[b]_i$ are matrices of constants to be determined.

The recursive evaluation, although in general only approximate, makes the analysis of soil-structure interaction in the time domain competitive with that performed in the frequency domain (complex response analysis which is, however, only applicable to a linear (total) system).

The choice of a recursive equation is, in general, not unique and many possibilities exist. Various procedures to determine the recursive coefficients are described in detail in Ref.2 and Ref.3 and are summarized in the text book Ref.1 and in Ref.4. These references also contain a literature survey. The recursive equations are derived based on the stiffness formulation, and the simple one-degree-of-freedom systems are used to illustrate the procedure. The references mentioned above have to be consulted to fully understand the following sections.

It is the aim of this paper to present applications of the recursive evaluation based on the flexibility formulation to multi-degree-of-freedom systems. Each coefficient of the dynamic-flexibility matrix is treated separately, enabling the procedures developed for the one-degree-of-freedom system to be used. First, the interaction forces of a rigid prism foundation embedded in a half-space for a prescribed displacement are calculated, whereby each dynamic-flexibility coefficient in the frequency domain is approximated as a ratio of two polynomials. Second, the partial uplift of a structure basemat resting on a half-space for a seismic excitation is examined as an example of a nonlinear soil-structure-interaction analysis. In this example, the dynamic-flexibility coefficients in the time domain are interpolated piecewise (segment approach). It should be stressed that after introducing the approximation in the flexibility coefficients either in the frequency or in the time domain, the so-called z-transformation leads to the recursive coefficients without any other approximations.

RIGID PRISM FOUNDATION

A massless rigid square foundation which forms a prism embedded in an elastic half-space is examined (Fig.2). The length is denoted as 2b and the embedment as e. The ratio e/b is selected as 0.5. The shear-wave velocity and Poisson's ratio of the half-space are denoted as c_s and $\nu=0.4$. The interaction moment (reaction) $R_r(t)$ acting at the centre of the basemat is calculated caused by a prescribed rotation $\psi(t)$ applied at the same location. $\psi(t)$ is a rounded triangular pulse, expressed in dimensionless time $\bar{t}=tc_s/b$ with $\bar{t}_0=2.5$ as (Fig.6).

$$\psi(\bar{t}) = \frac{\Psi_0}{2}\left[1-\cos\left(2\pi\frac{\bar{t}}{\bar{t}_0}\right)\right] \quad 0<\bar{t}\le\bar{t}_0 \quad (4a) \qquad \psi(\bar{t})=0 \quad \bar{t}>\bar{t}_0 \quad (4b)$$

The real and imaginary parts of the dynamic-flexibility coefficients in the frequency domain $F(a_0)$ calculated based on the boundary-element method are shown as dots in Fig.3. $a_0=\omega b/c_s$ is the dimensionless frequency, and K the static value. The subscripts h and r denote the horizontal and rotational directions.

As discussed in Ref.3, each dynamic-flexibility coefficient is approximated as a ratio of two polynomials in ia_0.

$$F(ia_0) = P(ia_0)/Q(ia_0) = K\left(1+\sum_{j=1}^{M-1} p_j (ia_0)^j\right)\Big/\left(1+\sum_{j=1}^{M} q_j (ia_0)^j\right) \tag{5}$$

The degree of the polynomial in the numerator is selected as one less than that in the denominator which is M.

The 2M-1 coefficients p_j, q_j, which are real, in eq.5 are determined using a curve-fitting technique based on the least-squares method. Great care must be taken in the details of the curve-fitting, especially when selecting M, to achieve a stable system. The 8 complex values shown as dots in Fig.3 in the range $0<a_0<4$ and the asymptotic value for $a_0\to\infty$ are used in the least squares method. The asymptotic value can be determined analytically, as in the limit one-dimensional wave propagation in the direction perpendicular to the vibrating surface that takes place (Ref.1). For instance, for rocking, the dynamic-stiffness coefficient is equal to

$$\lim_{a_0\to\infty} S_{rr}(a_0) = \left[\frac{(2b)^4}{12}\rho c_p + 2b^2 2be\rho c_s + 2\cdot 2b\frac{e^3}{3}\rho c_p + 2\cdot\frac{2}{3}(be^3+eb^3)\rho c_s\right] ia_0 \tag{6}$$

ρ and c_p are the mass density and the dilatational-wave velocity. The first term corresponds to the contribution of the basemat (P-waves) and the other three terms to those of the side walls (P- and S-waves). The asymptotic value of the dynamic flexibility coefficients follows from the inverse of that of the total dynamic-stiffness matrix.

Selecting M=5 for rocking results in the curves shown in Fig.4a for the range $0<a_0<8$, the roots of $Q(ia_0)$ are equal to $-2.84\pm1.42i$, $-1.30\pm0.79i$, $+4.63$. For stability, the real parts of all roots must be negative, which is not the case. M=3 with the curves shown in Fig.4b leads to the roots $-1.34\pm0.72i$, -6.22, which correspond to a stable system. As can be seen from Fig.4, the two curves differ slightly outside the range used for the curve fitting (real part, $a_0>6$).

The curves after curve fitting for the 3 dynamic-flexibility coefficients are shown as solid lines in Fig.3. M=5, 3, and 4 are used for the horizontal, rocking and coupling terms, respectively.

The dynamic-flexibility coefficients in the time domain are plotted in Fig.5. The poles of the z-transform of each flexibility coefficient are also indicated for $\Delta\bar{t}=0.125$. This pole is equal to the exponential function of the product of the root of $Q(ia_0)$ and $\Delta\bar{t}$. All poles lie inside the unit circle, which guarantees stability.

The interaction moment R_r calculated recursively with $\Delta\bar{t}=0.125$ is plotted in dimensionless form in Fig.7. The convolution integral leads to a non-zero response also in the range where the applied loading is zero ($\bar{t}>\bar{t}_0=2.5$).

PARTIAL UPLIFT OF BASEMAT OF REACTOR BUILDING

The partial uplift of the basemat of a typical nuclear reactor building on a half-space is investigated for severe earthquake excitation. The main dimensions are shown in Fig.8. The half-space has a shear-wave velocity 500m/s, a mass density 2000kg/m^3, Poisson's ratio 1/3 and a damping factor 0.02. The building is modeled by a lumped-mass model with 27 degrees of freedom after the static condensation. The foundation is assumed to be a strip foundation divided into 15 square boundary elements with piecewise constant normal and shear stresses. In each element two degrees of freedom(u,w) occur.

The flexibility coefficients ($F_{uu}(t)$, $F_{ww}(t)$) are calculated by integrating the well-known three-dimensional flexibility influence functions (Ref.1) specially and temporally. The foundation is assumed to be rigid, and the smoothed base condition ($F_{uw}(t)=0$) is applied.

To derive the recursive equations for the interaction forces the flexibility coefficients are divided into segments. In each segment, the function is approximated by the product of a polynomial and an exponential function. In Figs.9 and 10 two components of the vertical and horizontal flexibility coefficients calculated by segment approach for the elements with the numbers shown in Fig.8 are compared with the exact ones. The time increament Δt is selected as 0.001s. An approximation by 5 segments shows good agreement.

The EL CENTRO (1940 NS) earthquake scaled to 0.5g is applied as a horizontal excitation. The response analysis of 3s duration (0.6-3.6s) with a Δt=0.001s is performed, resulting in a total number of time steps N^t=3000. Denoting the number of boundary elements as N^s, the number of the bounded segments as N, the nember of time steps in the i-th segment of kj-component as $n_{kj:i}$, the number of operations in evaluating interaction forces is formulated as

$$3N^t\cdot 2(N^s)^2+2\sum_{s=1}^{N^s}\sum_{j=1}^{N^s}\sum_{i=1}^{N}4\left(N^t-n_{kj\cdot i}\right) \qquad (7)$$

Assuming $N^t \gg n_{kj\cdot i}$, this expressin can be written as $N^t 7N\cdot 2(N^s)^2$. In contrast the direct evaluation leads to $1/2\,(N^t)^2\, 2(N^s)^2$ operations. Denoting the number of time steps of the non-negligible part of the flexibility coefficient as $\tilde{N}^t$, the latter can be formulated as $\tilde{N}^t N^t 2(N^s)^2$. In this case, adopting N=5 and an average $\tilde{N}^t \simeq 60$ results in only about a 60% reduction in computational effort. But it should be stressed that the recursive evaluation leads to a significant reduction in case of a 2-dimensional problem, whereby the flexibility coefficients show the remarkable "tail" as can be seen in Fig.11($\tilde{N}^t \simeq N^t$), and in case of the layered half-space. The storage requirement is also reduced in the recursive evaluation. The segment approach needs $3\cdot 2(N^s)^2 + 2N^s\cdot 4(t_N/\Delta t + 4)$ storage units, denoting the maximum beginning time of the N-th segment as t_N . In contrast the direct evaluation needs $N^t\cdot 2N^s$ units.

The earthquake response is calculated by using the approximated flexibility coefficients. The comparison of the nonlinear response with partial uplift of the basemat and the linear one indicates that the accelerations (Fig.12) are not drastically affected although significant uplift occurs (Fig.13).

REFERENCES

1. Wolf J. P., "Soil-Structure-Interaction Analysis in Time Domain", Prentice-Hall, 1988.
2. Wolf J. P. and Motosaka M., "Recursive Evaluation of Interaction Forces of Unbounded Soil in the Time Domain", accepted for publication in Earthquake Engineering and Structural Dynamics.
3. Wolf J. P. and Motosaka M., "Recursive Evaluation of Interaction Forces of Unbounded Soil in the Time Domain from Dynamic-Stiffness Coefficients in Frequency Domain", accepted for publication in Earthquake Engineering and Structural Dynamics.
4. Motosaka M., "Study on Dynamic Soil-Structure-Interaction Analysis for Embedded Structure", Doctoral Dissertation, Tohoku University, Sendai, 1988 (in Japanese).

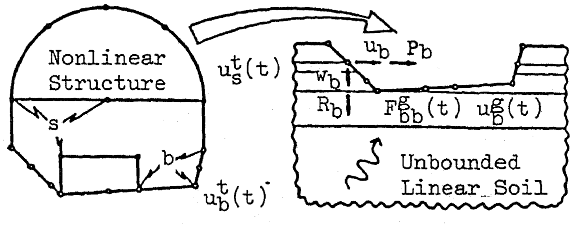

Fig.1 Substructure Method in Time Domain

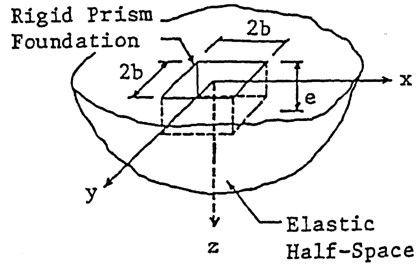

Fig.2 Rigid Prism Foundation Embedded in Elastic Half-Space

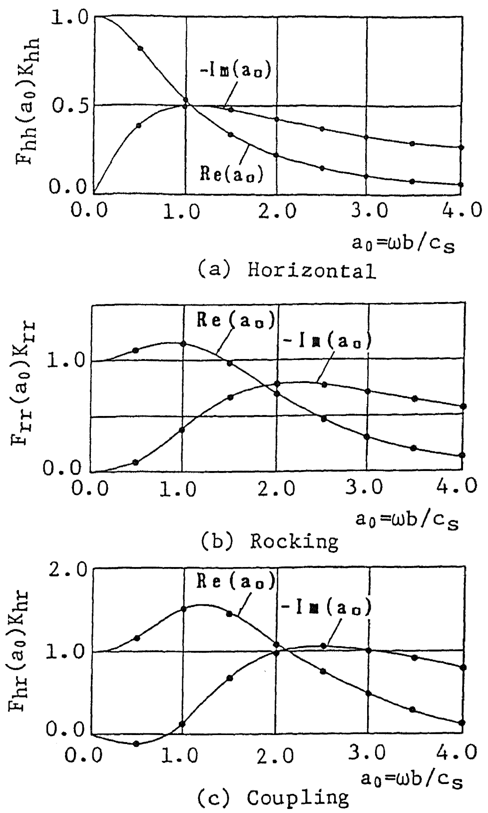

Fig.3 Dynamic-Flexibility Coefficients in Frequency Domain

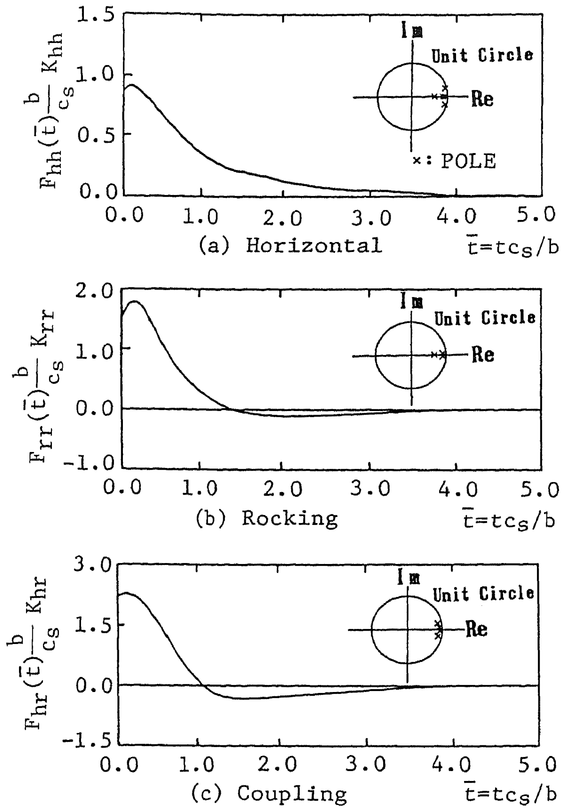

Fig.5 Dynamic-Flexibility Coefficients in Time Domain and Location of Poles in z-Domain ($\Delta\bar{t}$=0.125)

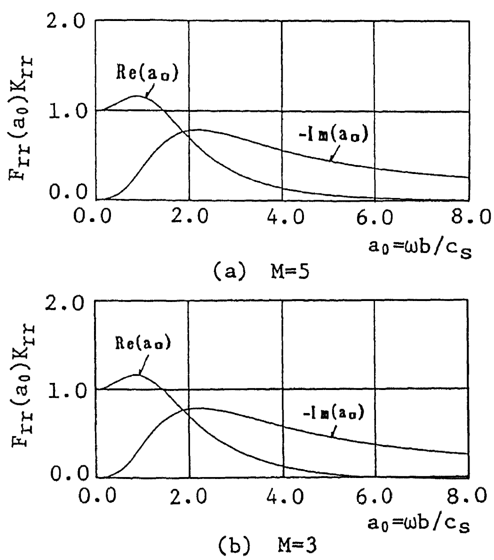

Fig.4 Influence of Degree of Polynomial in Denominator of Dynamic-Rocking Flexibility Coefficients

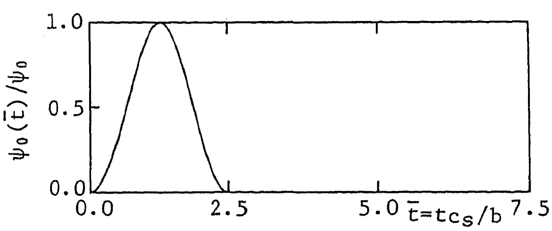

Fig.6 Prescribed Rotation of the Foundation

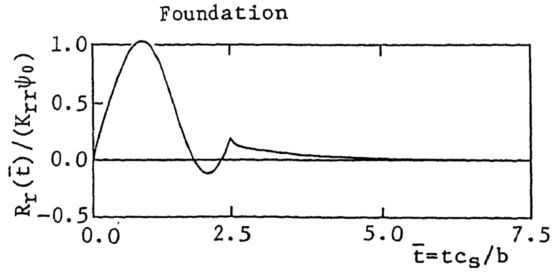

Fig.7 Rocking Interaction Moment

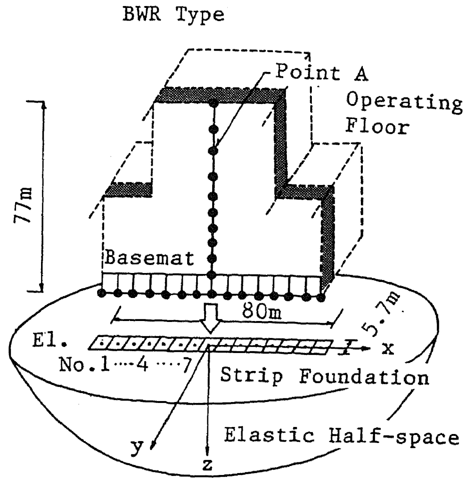

Fig.8 Reactor Building on Half-space

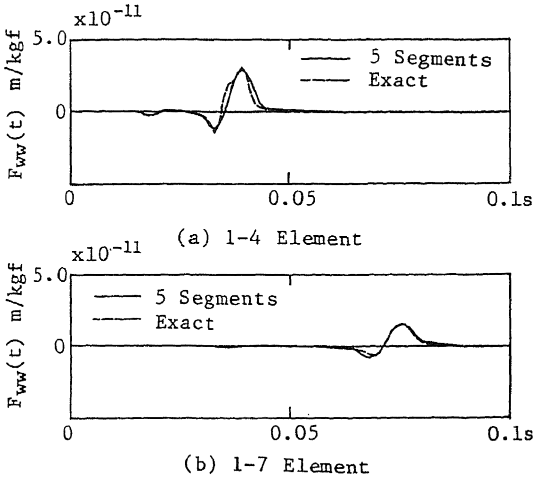

Fig.9 Vertical Flexibility Coefficients by Segment Approach

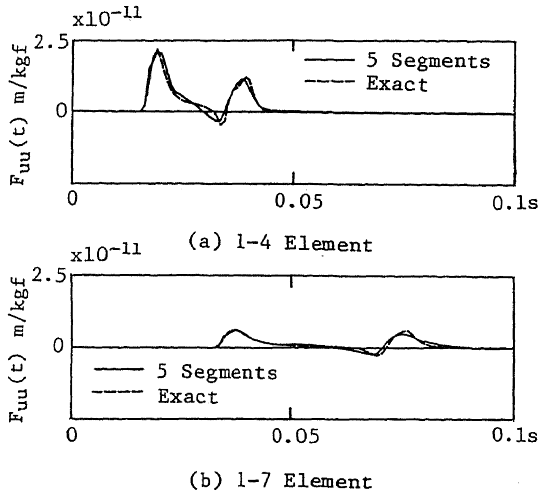

Fig.10 Horizontal Flexibility Coefficients by Segment Approach

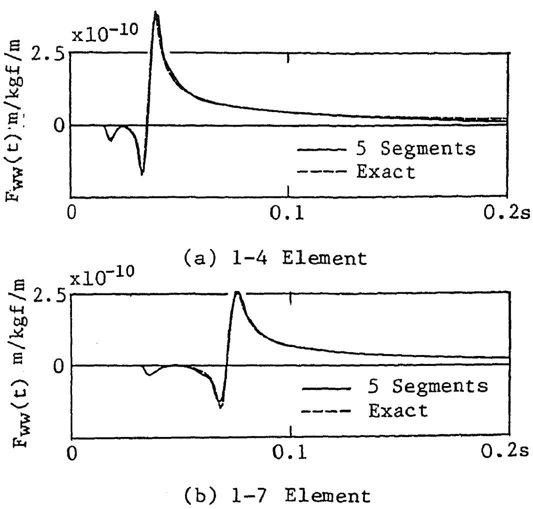

Fig.11 2-dimensional Vertical Flexibility Coefficients by Segment Approach

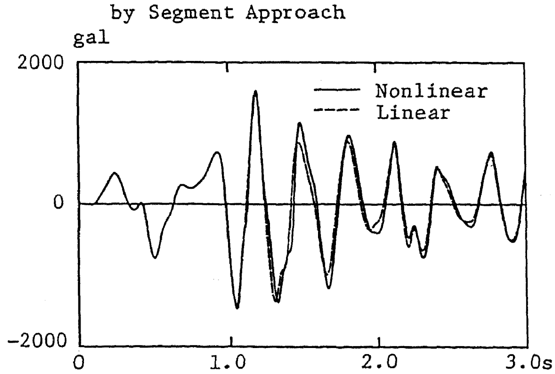

Fig.12 Time History of Acceleration in Point A

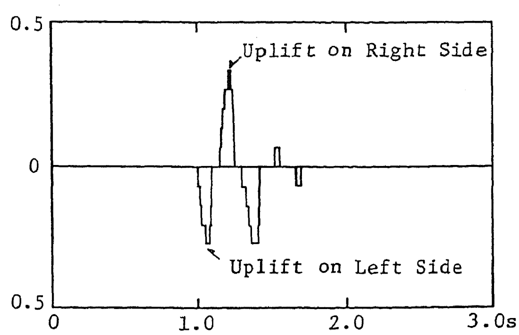

Fig.13 Time History of Uplift Ratio